Identification of FTIR Bands Due to Internal Water Molecules around the Quinone Binding Sites in the Reaction Center from *Rhodobacter sphaeroides*[†]

Tatsuya Iwata,[‡] Mark L. Paddock,[§] Melvin Y. Okamura,[§] and Hideki Kandori*,[‡]

Department of Frontier Materials, Nagoya Institute of Technology, Showa-ku, Nagoya 466-8555, Japan, and Department of Physics, University of California at San Diego, 9500 Gilman Drive, La Jolla, California 92093

Received October 24, 2008; Revised Manuscript Received December 22, 2008

ABSTRACT: The bacterial reaction center (RC) is a membrane protein complex that performs photosynthetic electron transfer from a bacteriochlorophyll dimer to quinone acceptors Q_A and Q_B. Q_B accepts electrons from the primary quinone, Q_A, in two sequential electron transfer reactions coupled to uptake of a proton from solution. It has been suggested that water molecules along the proton uptake pathway are protonated upon quinone reduction on the basis of FTIR difference spectra [Breton, J., and Nabedryk, E. (1998) *Photosynth. Res. 55*, 301−307]. We examined the possible involvement of water molecules in the photoreaction processes by studying ^{18}O water isotope effects on FTIR difference spectra resulting from formation of Q_A^- and Q_B^-. Continuum bands in D_2O due to Q_B^- formation in the 2300−1800 cm^{-1} region did not show spectral shifts by ^{18}O water in the wild-type (WT) RC, suggesting that these bands do not originate from (protonated) water. In contrast, the Q_B^-/Q_B spectrum of the EQ-L212 mutant RC showed a spectral shift of a band near 2100 cm^{-1} due to ^{18}O water substitution, consistent with protonation of internal water. FTIR shifts due to ^{18}O water were also observed following formation of Q_A^- and Q_B^- in the spectral region of 3700−3500 cm^{-1} characteristic of weakly hydrogen bonded water. The water responsible for the Q_B^- change was localized near Glu-L212 by spectral shifts in mutant RCs. The weakly hydrogen bonded water perturbed by quinone reduction may play a role in stabilizing the charge-separated state.

The photosynthetic bacterial reaction center (RC)[1] is a membrane protein complex with redox components that works in cooperation with the cytochrome bc_1 complex as a light-driven proton pump, transferring protons across biological membranes from the cytoplasmic side to the periplasmic side. The RC performs photochemical electron transfer from the bacteriochlorophyll dimer (P) through a series of electron donor and acceptor molecules to the secondary quinone, Q_B. Q_B accepts electrons from the primary quinone, Q_A, in two sequential electron transfer reactions. The second electron transfer to Q_B is coupled to the uptake of two protons from the cytoplasmic side, leading to the formation of the dihydroquinone Q_BH_2 that diffuses out of the RC (reviewed in refs *1* and *2*). The oxidation of the reduced quinone releases protons across the membrane, resulting in a proton gradient that is essential for ATP synthesis.

In the photosynthetic RC of purple bacteria, Q_B is buried in the protein away from the water surface. Thus, a pathway for proton transfer must be present to enable protons to penetrate to the Q_B site. The crystal structure of the RC from *Rhodobacter sphaeroides* shows that Q_B is surrounded by a cluster of acidic and polar amino acid residues (Glu-L212, Asp-L213, and Ser-L223) and water molecules which can facilitate transfer of a proton to Q_B. In addition, hydrophilic pathways which contain protonatable amino acid residues (Asp-M17, Asp-L210, His-H126, and His-H128) and water molecules are observed leading from the cytoplasm to the Q_B binding site (*3*−*6*) (Figure 1). The role of the carboxylic acid residues has been demonstrated by site-directed mutation, which results in reduced rates of proton uptake (*7*−*15*).

Light-induced electron transfer to form Q_A^- and Q_B^- results in proton uptake from solution (*16, 17*). Under these conditions, the reduced quinone has been found to be in the anionic semiquinone state (*18, 19*), indicating that the proton must be bound to some other molecule in the protein. The nature of the proton binding sites in RCs has been extensively studied by light-induced Fourier transform infrared (FTIR) spectroscopy (for a recent review, see ref *20*). The protonation of glutamic acid and aspartic acid results in absorption bands in the 1770−1700 cm^{-1} region due to C═O stretching vibrations of the protonated acid. Although considerable proton uptake is expected on the basis of electrostatic calculations (*21*−*26*), only one carboxylic acid, Glu-L212, was observed to change protonation state upon Q_B^- formation.

However, the intermediate states for proton uptake from the cytoplasmic side to the inside of the RC remain unclear because the protonation of internal groups is not observed except for Glu-L212 upon the reduction of Q_B (*27*−*31*). One

[†] This work was supported by grants from Japanese Ministry of Education, Culture, Sports, Science, and Technology to H.K. (19370067, 20044012, and 20050015) and from the National Institutes of Health to M.Y.O. (GM 41637).

* To whom correspondence should be addressed. Phone and fax: 81-52-735-5207. E-mail: kandori@nitech.ac.jp.

[‡] Nagoya Institute of Technology.

[§] University of California at San Diego.

[1] Abbreviations: RC, reaction center; Q_A, primary quinone; Q_B, secondary quinone; FTIR, Fourier transform infrared; BR, bacteriorhodopsin.

10.1021/bi801990s CCC: $40.75
Published on Web 01/22/2009

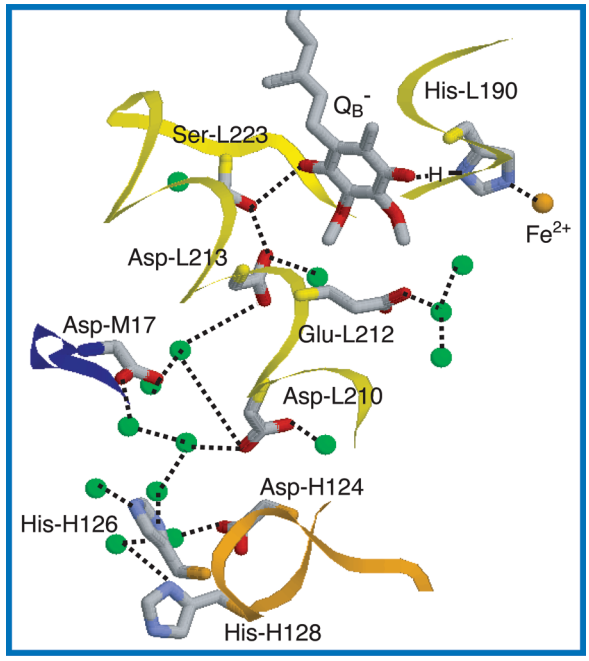

FIGURE 1: Structure of the Q_B binding site of the reaction center of *Rb. sphaeroides* in the $P^+Q_B^-$ state [PDB entry 1DV3 (*5*)]. Peptide backbones are shown as ribbons, where L, M, and H subunits are colored yellow, blue, and orange, respectively. Quinone and amino acid side chains are shown as stick drawings. Green spheres represent water molecules. Dotted lines show putative hydrogen bonds and coordinate bond.

puzzle is the observation that in some cases proton uptake is observed under conditions where no protonation of carboxylic residues is measured by FTIR. For instance, EQ-L212 mutant RCs lacking Glu-L212 display proton uptake in the Q_B^- state (*32*) but do not have increased FTIR bands in the carboxylic acid region. In addition, FTIR carboxylic acid protonation signals are not observed in the RC of *Blastochloris viridis* (*33*). How is proton uptake into the protein carried out without protonation of acid side chains?

One possibility is that an internal water molecule, in an ionic environment surround by carboxylic acids, serves as a protonated transient or stable intermediate in the proton transfer chain. Although it is likely that water molecules are commonly used to bridge transfer between proton donor and acceptor groups, serving as transient intermediates, it is less certain if water becomes stably protonated to form either Eigen (H_3O^+) (*34*) or Zundel cations ($H_5O_2^+$) (*35*). In the RC, several water molecules are observed near carboxylic acid groups in X-ray crystal structures that provide a connection between internal amino acids and allow for the formation of a contiguous hydrogen bonding network from the cytoplasmic surface to the internal catalytic Q_B site (Figure 1). Breton and Nabedryk interpreted H−D exchangeable IR signals in the 2800−1900 cm^{-1} region to be due to proton movement within a highly polarizable hydrogen bonded web, possibly involving water protonation (*36*). Hermes et al. observed similar signals in the DN-L210 mutant by time-resolved FTIR studies which were ascribed to protonation of internal water molecules due to the observed vibration frequency (*37*). Indeed, in bacteriorhodopsin (BR), a light-driven proton pump, protonation of internal water molecules (Zundel cation, $H_5O_2^+$) has been proposed as a proton release group detected in the 2000−1800 cm^{-1} region (*38, 39*). However, bands in this region are not by themselves sufficient evidence of protonated water. In BR, the O−H stretching vibration of the water molecule that bridges positive and negative charges appears at 2800 cm^{-1} (*40*−*42*), which forms an unusually strong hydrogen bond. Recently, we have further shown that the continuum band at 2000−1800 cm^{-1} in BR contains vibration of water by use of ^{18}O water (*43*). As shown for BR, conclusive assignment of a water band requires the use of an identifiable and specific isotopic substitution of the water molecules.

In this study, we examined the possible involvement of water molecules in the photoreaction processes of the RC by studying ^{18}O water isotope effects on native and EQ-L212 mutant RCs. Previously, we have shown the importance of internal water molecules in the proton transfer processes of bacteriorhodopsin (BR) by means of isotope water edited FTIR spectroscopy (*40*−*42*; reviewed in refs *44* and *45* and references therein). FTIR spectroscopy is a powerful tool for detecting changes in the hydrogen bond environment as well as the protonation state of internal groups. Here our goal is to detect structural changes in internal water molecules accompanied by the reduction of quinones in the RC. We developed conditions for water substitution of RCs in dry-hydrated films that produced the same FTIR signals as in solution. The changes in O−H (or O-D) stretching vibrations were examined in RC films hydrated with either H_2O or D_2O upon the reduction of Q_A or Q_B. D_2O substitution is useful for shifting O−D stretching vibrations into a region away from other interfering bands. The observed bands were assigned to water vibrations by measuring shifts due to substitution of ^{18}O for ^{16}O.

We studied the broad continuum bands in the 2950−2200 cm^{-1} region (in H_2O) and from 2300 to 1800 cm^{-1} (in D_2O) which have been proposed to contain contributions from protonated water. We did not observe an ^{18}O-shifted band in wild-type (WT) RCs in either H_2O or D_2O, suggesting that the bands in this region do not originate from (protonated) water. In contrast, we observed an ^{18}O spectral shift expected for a water band near 2100 cm^{-1} in D_2O for the EQ-L212 mutant RC upon formation of Q_B^-. This band is in a region expected for a protonated water molecule and is consistent with the proposal that protonated water is a stable species in proton transfer in the RC. We also examined the isotope shifts of bands in the region of the spectrum where weakly hydrogen bonded water vibrations are observed (3700−3500 cm^{-1} in H_2O or 2700−2400 cm^{-1} in D_2O). This region of the spectrum is relatively free of interference due to absorption of bulk water which has normal hydrogen bonding and is thus shifted to lower vibrational frequencies. Isotope-shifted bands were observed in WT RCs after either formation of Q_A^- and Q_B^-, indicating the presence of weakly hydrogen bonded water molecules near both Q_A and Q_B whose spectra are perturbed by quinone reduction. The water bands shifted due to Q_B^- formation were found to be perturbed in EQ-L212 RCs, indicating that this water is located near Glu-L212. The possible role of these water molecules is discussed.

MATERIALS AND METHODS

The construction of the site-directed mutant EQ-L212, DN-L213, and SA-L223 was previously reported (*7, 11, 12*). The purification of RCs was carried out as described in ref *11*.

RCs were dialyzed against dialysis buffer [10 mM Tris·HCl (pH 8), 0.1 mM EDTA·2Na, 5 mM NaCl, and 0.02% (w/v) dodecyl maltopyranoside]. Fifteen microliters of RC (70−100 μM) and 5 μL of reducing reagent mixture [10 mM sodium ascorbate, 20 mM 2,3,5,6-tetramethyl-*p*-phenylenediamine in 10 mM Tris·HCl (pH 8), 1 mM EDTA·2Na, and 0.025% (w/v) *N*,*N*-dimethyldodecylamine *N*-oxide] were mixed. For Q_A measurement, terbutryn was added to a final concentration of 100 μM. For Q_B measurement, 10 μL of ubiquinone-10 (1 mg/mL in ethanol) was added the RC mixture. The RC mixtures were put on a BaF_2 window and dried by aspiration. The RC films were rehydrated by placing ~1 μL of a 20% (v/v) glycerol/water mixture (H_2O or $H_2{}^{18}O$) (Taiyo Nioopn Sanso; 98% ^{18}O) aside (99% relative humidity) (*46*).

H−D exchange was carried out by diluting the RC sample with dialysis buffer prepared in D_2O and concentrating with an Amicon YM-30 device (Millipore) three times. The RC in D_2O buffer was incubated for 16 h at 293 K according to the method described in ref *14*. For Q_A and Q_B measurements, the same reagents were added as D_2O-treated samples and dried on a BaF_2 window. The RC films were rehydrated with 20% (v/v) glycerol-$(OD)_3$ (Cambridge Isotope Laboratories; 98% D) and D_2O (Spectra Gases; 99% D) or $D_2{}^{18}O$ (Icon Isotopes; 99% D, 95% ^{18}O).

Light-induced Q_A^-/Q_A difference spectra were measured at 283 K under continuous illumination with >700 nm light (R69 and C40B, Asahi Thechno Glass) with a 1 kW tungsten lump (*47*). Light intensity was decreased to 1% by the use of the ND1 filter for the Q_B^-/Q_B measurements of WT (*48*) and SA-L223, and 0.5% (ND1 and ND50) for the measurements of EQ-L212 and DN-L213 because bands from Q_A^- appeared by the illumination using the ND1 filter (data not shown). For FTIR spectra, 256 interferograms at 2 cm^{-1} resolution were recorded during and before illumination and after and during illumination. By subtracting difference spectra after and during illumination from difference spectra during and before illumination, we efficiently eliminated baseline drift. Typical signal intensities were 0.003 at 1467 cm^{-1} for the WT Q_A^-/Q_A spectra, 0.0015 at 1478 cm^{-1} for the Q_B^-/Q_B spectra of WT and SA-L223, and 0.0006 at 1478 cm^{-1} for the Q_B^-/Q_B spectra of EQ-L212 and DN-L213; 80−100 recordings were averaged, each of which exhibited a similar spectral trend.

RESULTS

Q^-/Q Difference FTIR Spectra of the Rehydrated RC Films. The FTIR difference spectra in rehydrated films were compared to the spectra obtained in solution to determine if changes due to sample differences were observed. Panels a−c of Figure 2 show the Q_A^-/Q_A and Q_B^-/Q_B difference spectra of the WT and Q_B^-/Q_B difference spectra of the EQ-L212 mutant RC films in the 1800−1200 cm^{-1} region, respectively. A characteristic positive band at 1467 cm^{-1} is observed in the Q_A^-/Q_A spectrum (Figure 2a), which comes from a C⋯O stretch (*49, 50*) semiquinone. The bands at 1735 (−)/1729 (+) cm^{-1} are reported to the 10a-ester C═O stretch of bacteriopheophytin on the A side (*51*). The negative band at 1670 cm^{-1} is assigned to the amide I C═O stretch (*49*). These are identical to Q_A^-/Q_A spectra previously reported (*47, 49−51*). Similarly, a positive peak at 1479 cm^{-1} for the Q_B^-/Q_B spectrum (Figure 2b) comes from C⋯O/C⋯C stretching

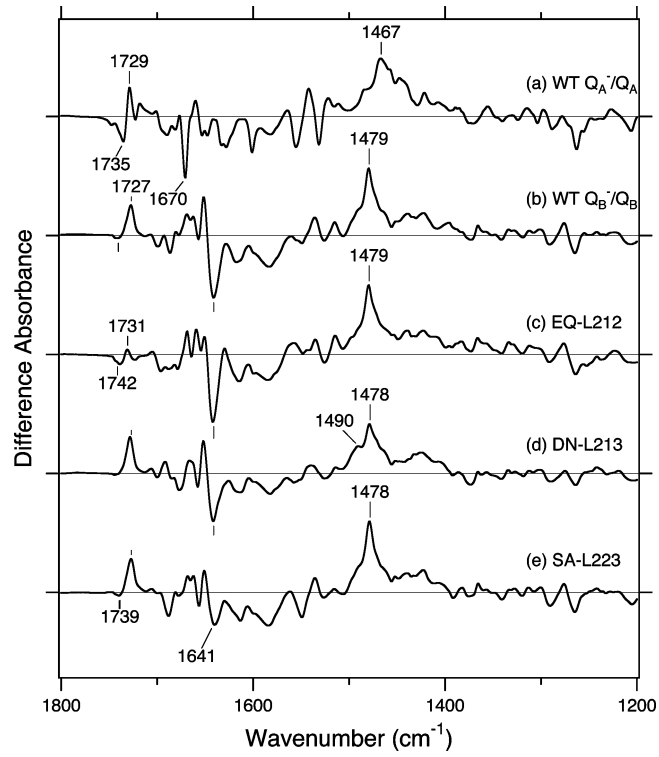

FIGURE 2: Light-induced Q^-/Q difference FTIR spectra of *Rb. sphaeroides* RCs in the 1800−1200 cm^{-1} region. Q_A^-/Q_A spectrum of WT (a) and Q_B^-/Q_B spectra of WT (b), EQ-L212 (c), DN-L213 (d), and SA-L223 (e). Averaged spectra a−e were multiplied by 0.51, 1, 1.91, 1.40, and 1.62, respectively, for the sake of comparison. One division of the *y*-axis corresponds to 0.003 absorbance unit.

bands of semiquinone (*52, 53*). The negative peak at 1641 cm^{-1} originates from C═O groups of neutral Q_B (*52, 53*). The positive band at 1728 cm^{-1} comes from the C═O group of the protonated carboxylic acid side chain of Glu-L212 (*27*), which disappeared in EQ-L212 (Figure 2c). Instead, smaller bands at 1739 (−)/1731 (+) cm^{-1} remain. The bands are assumed to be a C═O stretch at 10a-ester in the bacteriopheophytin on the B side (*30*).

Thus, the similarity of these spectra to those from isolated RCs shows that there are no dramatic changes to the properties and protein responses of RCs in the dry-hydrated films. With most of the bulk water removed, we were now able to investigate higher frequencies.

Continuum Bands in the 2900−2200 cm^{-1} Region. The FTIR difference spectra due to quinone reduction were measured in the continuum region where bands due to protonated water have been proposed. Figure 3 shows Q^-/Q difference FTIR spectra of WT and EQ-L212 mutant RCs in the 2900−2200 cm^{-1} region. In the Q_A^-/Q_A spectrum of WT, there are positive peaks at 2818, 2756, 2709, 2611, and 2559 cm^{-1} (Figure 3a). Similarly, the Q_B^-/Q_B spectrum of WT has a main peak at 2613 cm^{-1} and small peaks at 2831, 2764, 2691, and 2559 cm^{-1} (Figure 3b), whose feature was quite identical in EQ-L212 (Figure 3c). The broad features were previously reported (*36, 54*) and were tentatively interpreted to involve highly polarizable hydrogen bonds involving cofactors, amino acids, and water. More recently, the broad feature of the Q_A^-/Q_A spectrum was shown to contain a contribution from the strongly hydrogen bonded N_π-H group of His-M219 (*55*). Contributions from protonated water molecules were

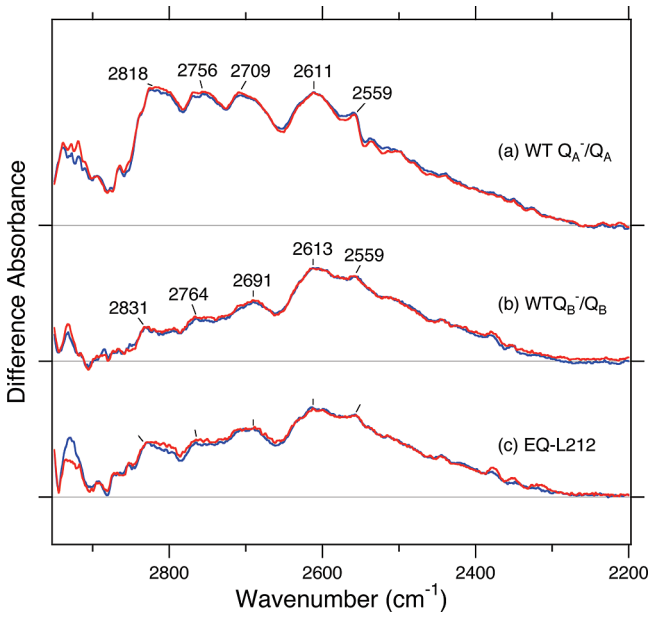

FIGURE 3: Light-induced Q^-/Q difference FTIR spectra of WT *Rb. sphaeroides* RCs in the 2950−2200 cm^{-1} region. Samples were hydrated with H_2O (red lines) or $H_2{}^{18}O$ (blue lines). Q_A^-/Q_A spectra of WT (a) and Q_B^-/Q_B spectra of WT (b) and EQ-L212 (c) are shown, which are taken from parts a−c of Figure 2, respectively. One division of the *y*-axis corresponds to 0.00045 absorbance unit.

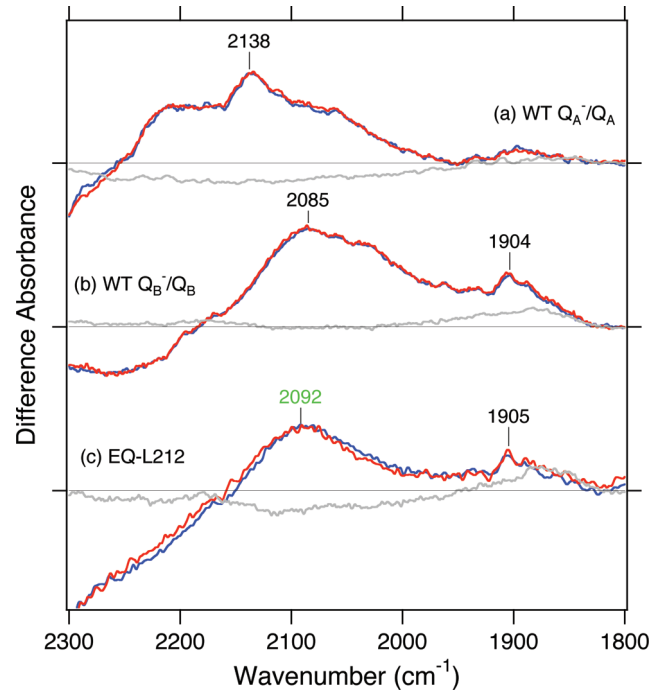

FIGURE 4: Light-induced Q^-/Q difference FTIR spectra of WT *Rb. sphaeroides* RCs in the 2300−1800 cm^{-1} region. Samples were hydrated with D_2O (red lines), $D_2{}^{18}O$ (blue lines), or H_2O (gray lines). Q_A^-/Q_A spectra of WT (a) and Q_B^-/Q_B spectra of WT (b) and EQ-L212 (c) are shown. One division of the *y*-axis corresponds to 0.00042 absorbance unit.

expected to produce spectral shifts of ∼8.5 cm^{-1} upon exchange with $H_2{}^{18}O$. However, the broad bands in the 2600 cm^{-1} region did not show any shift by hydration of $H_2{}^{18}O$ water (Figure 3, blue lines), preventing us from assigning some of the features to water. To investigate whether the spectral shifts are clearly observed for the Q^-/Q spectra, hydration by $D_2{}^{16}O/D_2{}^{18}O$ was carried out. The difference in the O−D stretching vibration of $D_2{}^{16}O$ and $D_2{}^{18}O$ is expected to be 15−18 cm^{-1}, which is larger than O−H stretches, even though the other signals appear in the same frequency region.

Assignment of Water Signals in the O−D Stretching Continuum Region (2300−1800 cm^{-1}). The FTIR difference spectra due to quinone reduction were measured in D_2O in the continuum region where the shifted protonated water bands should occur. Figure 4 compares the Q_A^-/Q_A and Q_B^-/Q_B spectra between hydration of $D_2{}^{16}O$ (red lines) and $D_2{}^{18}O$ (blue lines). The positive broad bands showed H−D exchange and downshifted to the 2300−1800 cm^{-1} region. The Q_A^-/Q_A and Q_B^-/Q_B spectra of WT possess peaks at 2138 cm^{-1} (Figure 4a) and at 2085 and 1904 cm^{-1} (Figure 4b), respectively. Parts a and b of Figure 5 show double-difference spectra between hydration of $D_2{}^{16}O$ and $D_2{}^{18}O$ in parts a and b of Figure 4, respectively. These spectra are identical to the baseline within the noise level. We thus concluded that there is no water O−D stretching signal in the 2300−1800 cm^{-1} region of the WT RC. Instead, as proposed for the Q_A^-/Q_A spectrum (*55*), the N−H (N-D) stretch of His may be involved in the spectra.

On the other hand, the Q_B^-/Q_B difference FTIR spectra of the EQ-L212 mutant showed a spectral shift was observed between $D_2{}^{16}O$ and $D_2{}^{18}O$ in the 2300−1800 cm^{-1} region (Figure 4c). Though the signal-to-noise ratios of EQ-L212 spectra were worse than those of WT because of the smaller intensity (see Materials and Methods), the positive peak at 2092 cm^{-1} (red line) shows a reproducible shift to a lower frequency in $D_2{}^{18}O$ (blue line). This is more obviously seen in the double-difference spectrum (black line in Figure 5c), which has a first-derivative shape indicating a peak shift. The difference spectrum was fitted by two Gaussian functions, whose peaks are located at 2110 and 2095 cm^{-1} (red and blue lines in Figure 5d). These spectra correspond to $^{16}O-D$ (red line) and $^{18}O-D$ (blue line) stretching vibrations of water. The remainder of the signal (black line in Figure 5d) should correspond to other O−D or N−D stretch(es). The broad positive bands at 2300−1800 cm^{-1} of EQ-L212 *do* contain water stretching vibrations, but those of WT *do not*. The corresponding O−H stretch should be located at ∼2600 cm^{-1}, though the isotope shift was not clear (Figure 3c). In fact, the double-difference spectrum of the two spectra in Figure 3c is identical to the baseline within the noise level (data not shown). We infer that the isotope shift of ∼8.5 cm^{-1} for the water O−H stretch was not sufficient under the present experimental accuracy, but the isotope shift of the O−D stretch (isotope shift by 15−18 cm^{-1}) was observable.

Q^-/Q Difference FTIR Spectra in the 3700−3480 cm^{-1} Region. The FTIR difference spectra due to quinone reduction were measured in the spectral region where O−H vibrations due to weakly hydrogen bonded water molecules occur. Figure 6a shows Q_A^-/Q_A spectra of the WT RC in the 3700−3480 cm^{-1} region. The Q_A^-/Q_A spectrum hydrated with H_2O (red line) has peaks at 3664 (+), 3657 (−), 3622 (−), 3587 (−), 3501 (−), and 3488 (+) cm^{-1}. Of those, the bands at 3664 (+), 3657 (−), 3622 (−), and 3587 (−) cm^{-1} undergo spectral shifts of 10−11 cm^{-1} by the hydration of $H_2{}^{18}O$ (blue line), indicating that these bands originate from water stretching vibrations upon the formation of Q_A^-. The band at 3664 (+) cm^{-1} remains in the $H_2{}^{18}O$-hydrated

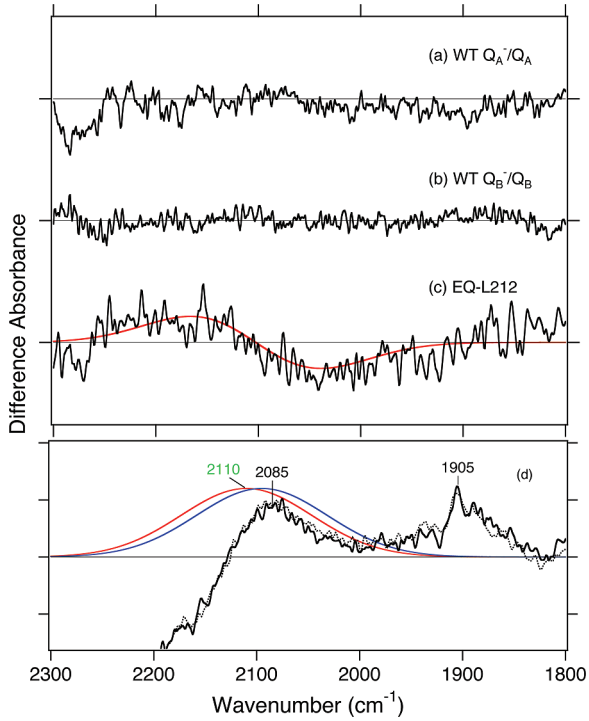

FIGURE 5: Double-difference spectra between $D_2{}^{16}O$ and $D_2{}^{18}O$ for Q_A^-/Q_A of WT (a), Q_B^-/Q_B of WT (b), and Q_B^-/Q_B of EQ-L212 (black line in c) in Figure 4. The red trace in part c shows the fitted spectrum by the difference spectrum of two Gaussian functions shown in part d (red and blue traces). The peak positions are 2110 (red line) and 2095 cm^{-1} (blue line), with the full width at half-maximum being 150 cm^{-1}. Black solid and dotted lines in part d show the difference spectra between those in Figures 4c and 5c (red and blue lines), respectively. One division of the *y*-axis corresponds to 0.000075 absorbance unit.

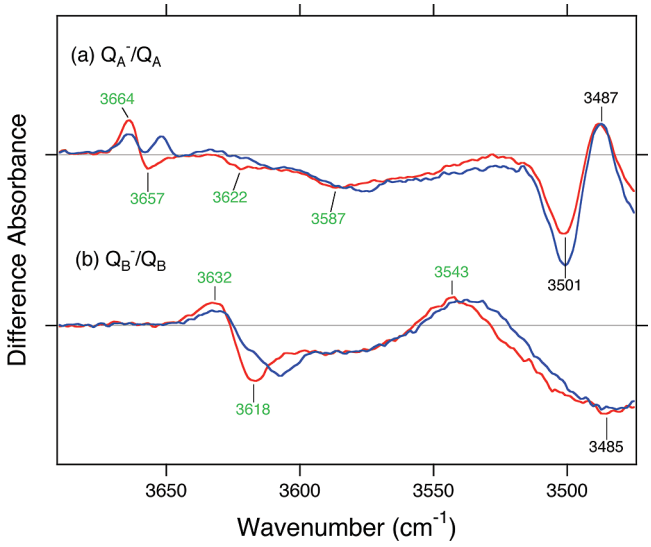

FIGURE 6: Light-induced Q_A^-/Q_A (a) and Q_B^-/Q_B (b) difference FTIR spectra of *Rb. sphaeroides* WT RCs in the 3700−3480 cm^{-1} region. Samples were hydrated with H_2O (red lines) and $H_2{}^{18}O$ (blue lines). One division of the *y*-axis corresponds to 0.0003 absorbance unit.

sample. This is probably because multiple signals appear at the same frequency region or because of incomplete substitution with $H_2{}^{18}O$. Since complete substitution was not expected, we decided to use the amplitude of the 3664 (+) cm^{-1} band as a measure of the remaining $H_2{}^{16}O$, the contribution of which should be subtracted by use of the $H_2{}^{16}O$ spectrum. The contribution of the $^{16}O-H$ stretch was estimated to be 50%.

The Q_B^-/Q_B spectrum hydrated with H_2O has peaks at 3632 (+), 3618 (−), 3543 (+), and 3485 (−) cm^{-1} and shows $H_2{}^{18}O$ isotope shifts at 3618 (−) and 3543 (+) cm^{-1} (Figure 6b). These shifted bands originate from water stretch vibrations. On the other hand, although the band at 3632 (+) cm^{-1} does not clearly shift, its amplitude is decreased by $H_2{}^{18}O$ hydration. As for Q_A^-/Q_A spectra, we assumed incomplete substitution of $H_2{}^{18}O$ as a measure of the level (∼50%) of $H_2{}^{16}O$ in the dried sample.

The signals appearing in this region represent weakly hydrogen bonded groups. Those water molecules are located in the hydrophobic environment or the hydrophilic environment, but the O−H stretch does not form a hydrogen bond. In either case, those water molecules are expected to be inside the protein. The substitution efficiency of the water ^{18}O whose O−H stretch appears in such an environment is approximately 50% by the operation of hydration. IR spectra could detect water molecules around quinones whose environments differ from each other. We can distinguish both Q^-/Q spectra in this frequency region clearly as well as in the 1800−1200 cm^{-1} region. The bands at 3501 (−) and 3487 (+) cm^{-1} in the Q_A^-/Q_A spectrum and at 3485 (−) cm^{-1} in the Q_B^-/Q_B spectrum, which did not show isotope shifts with $H_2{}^{18}O$, probably come from the O−H or N−H stretch of amino acid residues.

Mutational Effect at Glu-L212 for Q_B^-/Q_B Spectra in the 3700−3480 cm^{-1} Region. To localize the position of the weakly hydrogen bonded water molecules responsible for the spectral changes, we measured FTIR difference spectra in mutant RCs having changes to residues near the Q_B site. Figure 7a shows Q_B^-/Q_B spectra of EQ-L212 in the 3700−3480 cm^{-1} region. The spectrum has one negative and two positive peaks (Figure 7a, red line). They were assigned as water O−H stretches because the bands exhibited a downshift upon rehydration in $H_2{}^{18}O$ (Figure 7a, blue line). The overall spectral shapes look similar for WT and EQ-L212 RCs, but the peak frequencies are different. Figure 7d compares the EQ-L212 spectrum with the WT spectrum. The positive bands in the EQ-L212 spectrum shift to the higher frequency by 5 cm^{-1} compared with the WT spectrum. The negative peak showed a 2 cm^{-1} shift to a higher frequency. Because these bands were influenced by the mutation at Glu-L212, the water molecules are sensitive to small changes at L212 and are likely located near Glu-L212.

In contrast to the spectral changes observed in the Glu-L212 (EQ-L212) mutant RCs, mutations at Asp-L213 (DN-L213) and at Ser-L223 (SA-L223), both of which are essential for proton transfer to Q_B (Figure 1) (*8, 10*−*13*), showed only minor changes compared to the WT (Figure 7). Parts b and c of Figure 7 show Q_B^-/Q_B spectra of SA-L223 and DN-L213, respectively, in the 3700−3480 cm^{-1} region. The peaks were assigned as water O−H stretches by comparing spectra hydrated with $H_2{}^{16}O$ and $H_2{}^{18}O$ (red and blue lines in parts b and c of Figure 7). Parts e and f of Figure 7 compare mutant spectra with the WT spectrum. The spectrum of DN-L213 has peaks at 3632 (+) and bands at 3619 (−) and 3543 (+) cm^{-1} (Figure 7e). Though a negative band showed a 1 cm^{-1} shift compared with that of WT, it suggests that those water molecules are not influenced by the mutation at Asp-L213. Water bands appear at 3632 (+),

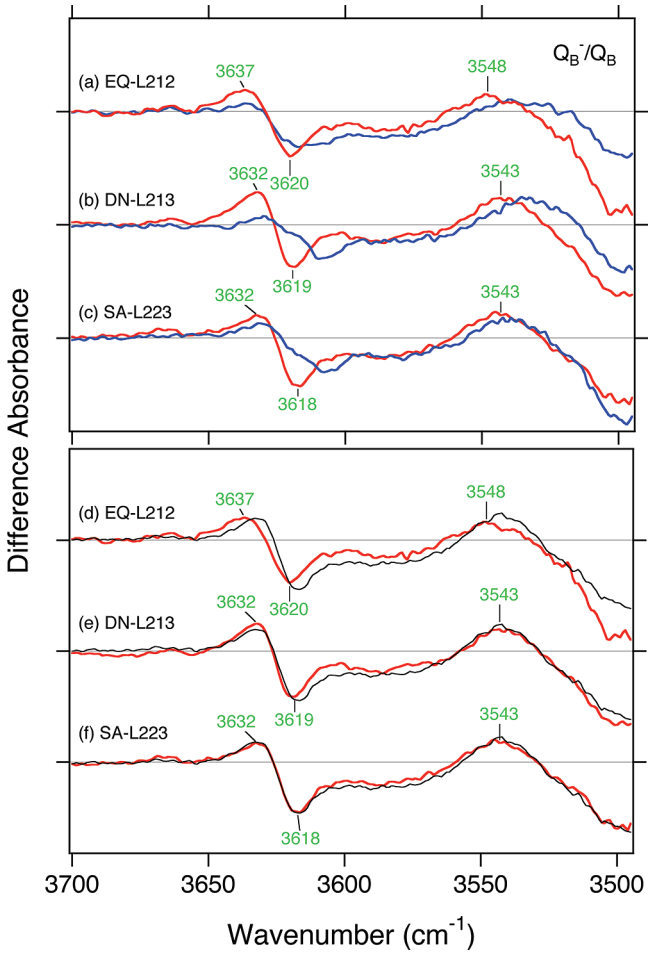

FIGURE 7: Light-induced Q_B^-/Q_B difference FTIR spectra of *Rb. sphaeroides* mutant RCs in the 3700−3490 cm^{-1} region. (a−c) Q_B^-/Q_B spectra of EQ-L212 (a), DN-L213 (b), and SA-L223 (c) hydrated with H_2O (red lines) or $H_2{}^{18}O$ (blue lines). (d−f) Q_B^-/Q_B spectra of EQ-L212 (d), DN-L213 (e), and SA-L223 (f) (red lines) are compared with the spectrum of WT (black lines). The samples were hydrated with H_2O. One division of the *y*-axis corresponds to 0.0003 absorbance unit. Labeled frequencies correspond to those identified as water stretching vibrations.

3618 (−), and 3543 (+) cm^{-1} for SA-L223, which are identical with those of WT (Figure 7f). These water bands are not influenced by the mutation at Ser-L223, suggesting that these water molecules are not located near Ser-L223. Thus, the observed water molecules are located in the region of Glu-L212.

Hermes et al. (*37*) reported the existence of a band of water at 3681 cm^{-1} for the DN-L210 mutant, but we could not find any bands in the 3700−3670 cm^{-1} region for the native or mutant RCs used in this study (Figures 6 and 7). The signal may be specific to the DN-L210 mutant.

Assignment of Water Signals in the O−D Stretching Vibration Region (2750−2390 cm^{-1}). The FTIR difference spectra were measured in D_2O in the spectral region for water molecules with weak hydrogen bonds. Parts a and b of Figure 8 show the Q_A^-/Q_A and Q_B^-/Q_B spectra of WT hydrated with D_2O (red lines) and $D_2{}^{18}O$ (blue lines) in the 2750−2390 cm^{-1} region. Gray spectra are Q^-/Q spectra hydrated with H_2O (Figure 3). Below the 2650 cm^{-1} region, the continuum bands disappear and new bands appear. The continuum bands show H−D exchange and are downshifted to ∼2100 cm^{-1} (Figure 4). New bands originate from X−D stretches shifted from the 3800−3200 cm^{-1} region. Q_A^-/Q_A spectra have

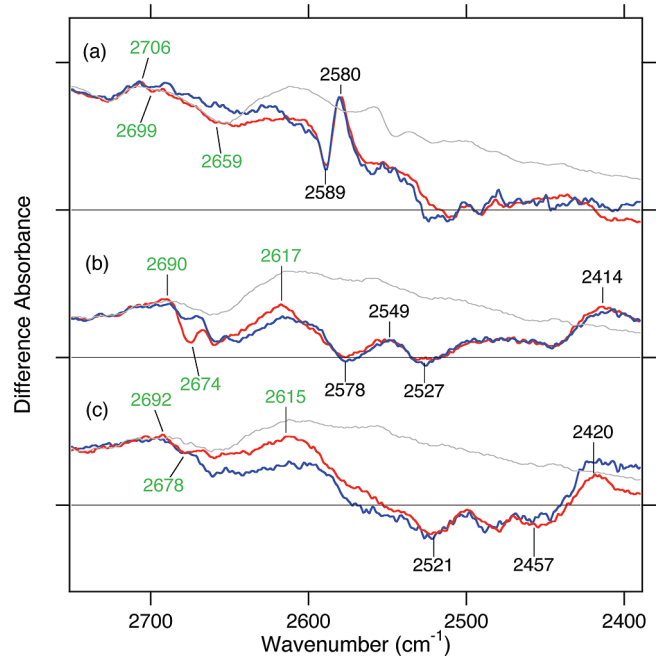

FIGURE 8: Light-induced Q^-/Q difference FTIR spectra of WT *Rb. sphaeroides* RCs in the 2750−2390 cm^{-1} region. Samples were hydrated with $D_2{}^{16}O$ (red lines), $D_2{}^{18}O$ (blue lines), and $H_2{}^{16}O$ (gray lines). Q_A^-/Q_A spectra of WT (a) and Q_B^-/Q_B spectra of WT (b) and EQ-L212 (c) are shown. One division of the *y*-axis corresponds to 0.00045 absorbance unit.

characteristic peaks at 2589 (−) and 2580 (+) cm^{-1}. These bands are shifted from 3501 (−) and 3487 (+) cm^{-1}, respectively (Figure 6a). Small bands at 2706 (+), 2699 (−), and 2659 (-) cm^{-1} exhibited spectral shifts in $D_2{}^{18}O$, which originate from water O−D stretches. These bands correspond to 3664 (+), 3657 (−), and 3587 (−) cm^{-1} bands in the O−H stretching vibration region (Figure 6a). The expected water O−D band corresponding to 3622 (−) cm^{-1} in the O−H stretch was not observed probably because the signal amplitude of the O−D stretch is small and masked by a remaining D_2O insensitive positive peak around 2700 cm^{-1}. Because no bands were observed in the 2580−2400 cm^{-1} region, we concluded that there are no water O−D stretches in this region.

The Q_B^-/Q_B spectrum has peaks at 2690 (+), 2674 (−), 2617 (+), 2578 (−), 2549 (+), 2527 (−), and 2414 (+) cm^{-1} (Figure 8b). Of those, the bands at 2690 (+), 2674 (−), and 2617 (+) cm^{-1} show a $D_2{}^{18}O$ isotope shift and correspond to the O−H stretches at 3632 (+), 3618 (−), and 3543 (+) cm^{-1}, respectively (Figure 6b). No water O−D stretches were observed in the 2600−2400 cm^{-1} region or in the Q_A^-/Q_A spectrum, and other peaks would originate from pigments or amino acid residues.

Figure 8c shows Q_B^-/Q_B spectra of EQ-L212 hydrated with $D_2{}^{16}O$ (red line) and $D_2{}^{18}O$ (blue line). The peaks at 2692 (+), 2678 (−), and 2615 (+) cm^{-1} originate from water O−D stretches and correspond to the O−H stretches at 3637 (+), 3620 (−), and 3548 (+) cm^{-1}, respectively. Other peaks at 2521 (−), 2457 (−), and 2420 (+) cm^{-1} did not exhibit a $D_2{}^{18}O$ isotope shift.

DISCUSSION

Continuum Bands in the WT and EQ-L212 Mutant. In this report, water vibrations were identified in reaction centers

from *Rb. sphaeroides* upon reduction of Q_A and Q_B using ^{18}O water substitution effects on O−H or O−D stretching frequencies. The broad positive bands at 2300−1800 cm^{-1} of EQ-L212 contain water stretching vibrations, but those of WT do not (Figure 4). The corresponding O−H stretch is probably located at ∼2600 cm^{-1}, though the isotope shift was not clear (Figure 3c). The water O−D stretch at 2110 cm^{-1} is even lower than the frequency of the bridged water (2171 cm^{-1}) in the Schiff base region of BR (*40*). What is the origin of such a strongly hydrogen bonded water band in EQ-L212? It may be possible that a water O−D group strongly associates with a negative charge such as Q_B^-, but if it does, we also expect it in the WT RC. Upon formation of Q_B^-, proton uptake from the aqueous phase occurs for both WT and EQ-L212 (*32*) and is expected on the basis of simple electrostatic attraction (charge compensation) and confirmed by electrostatic calculations (*21*−*26*). The proton acceptor for WT is Glu-L212 (*27, 28, 31*) as is clearly seen from the appearance of the C═O stretch at 1727 cm^{-1} (Figure 2b), but it has not been identified for EQ-L212. The appearance of a low-frequency peak due to a water molecule leads to the interpretation that the previously unidentified proton acceptor could be an internal water molecule(s) with the O−D stretch at 2110 cm^{-1} due to formation of D_3O^+ or $D^+(D_2O)_n$ (Figure 1). Low-frequency vibrations in this region of the spectrum due to a protonated water cluster have been observed in the gas phase (*56, 57*). The greater width of the water O−D band (150 cm^{-1}) versus that for the fixed water molecules in BR (70−80 cm^{-1} for the 2171 cm^{-1} band) (*40*) can be explained by delocalization of the proton among multiple water molecules. The location of protonated water could be in the region of acidic residues Asp-L213, Asp-M17, and Asp-L210 (Figure 1), where the protonated water could be stabilized by interactions with a cluster of negative charges due to carboxylic acid residues. Thus, it is conceivable that the band could be due to a protonated water inside the RC. In BR, the protonated water cluster has been proposed to be a proton release group on the basis of the broad IR band at 2000−1900 cm^{-1} (*38, 39*). This proposal was recently evidenced by the careful isotope measurement of water via time-resolved FTIR (*43*). Thus, water clusters inside proteins may function in protonation and deprotonation processes.

Then, what is the origin of the continuum bands which do not originate from water stretching (Figures 4a,b and 5d)? They more likely originate from N−D stretches which form strong hydrogen bonds. It was previously determined that the N−D stretch of the protonated Schiff base in the ground state of BR also appears at 2171 cm^{-1} (*58*). In the Q_A^-/Q_A FTIR difference spectra of photosystem II, multiple peaks in the 3000−2600 cm^{-1} region originate from strongly hydrogen bonded histidines (*59*). Including the result of Breton et al. (*60*), all bands in this IR region observed in the Q_A^-/Q_A spectrum could originate from the strongly hydrogen bonded N−H group of His-M219. Since similar peaks were also observed in the Q_B^-/Q_B difference spectrum, we assume that the bands originate from the N_π−H group which is positively charged or which forms strong hydrogen bonds with negatively charged groups. Therefore, it is possible that His-L190 (strongly hydrogen bonded with negatively charged Q_B^-) (Figure 1) is similarly a major contributor to the difference Q_B^-/Q_B IR spectrum. Such a strong hydrogen bond could be involved in the donation of a proton from Glu-L212 as well as the rearrangement of water molecules.[2]

Assignment of Water Molecules That Form Weak Hydrogen Bonds. Changes in FTIR spectra in the high-frequency region indicate the presence of weakly hydrogen bonded water molecules near both Q_A and Q_B. The water molecules responsible for changes due to formation of Q_B^- were localized around Glu-L212, which is involved in the donation of a proton to Q_B. Because the mutation of Asp-L213, which is next to Glu-L212, did not influence the water bands (Figure 7), it is likely that the water molecules that contribute to the IR spectrum must be located in a relatively small region around Glu-L212. It may be reasonable that the SA-L223 mutant does not affect the water structural changes upon formation of Q_B^- because Ser-L223 is not involved in the proton uptake pathway associated with the formation of Q_B^- (ref *2* and references within).

The spectral changes in this spectral region due to Q_B^- formation include two bands that appear and two bands that disappear. It seems reasonable to assume that these changes are due to the increase in the frequency of two O−H vibrations due to the presence of the negative charge on Q_B^- (although this is not proven). In principle, these spectral changes can be due to alterations of two weakly hydrogen bonded O−H groups in one water molecule or to two weakly hydrogen bonded O−H groups in two different water molecules. In the latter case, the other more strongly hydrogen bonded O−H group would have a lower frequency and be in the bulk water region not examined in this study.

Possible candidates for the weakly hydrogen bonded waters are found in X-ray crystal structures of the RC, such as the three water molecules near Glu-L212 seen in Figure 1. The central water molecule, hydrogen bonded to Glu-L212, has both protons in hydrogen bonds and is not a likely candidate; the two peripheral water molecules may have one or both protons in weak hydrogen bonding positions. The FTIR changes may be due to the changes in stretching frequency of one or two of these water molecules in response to the protonation of Glu-L212 and/or the negative charge on Q_B^-. Since spectral changes are still observed in EQ-L212 RCs where the L212 residue is always neutral, the main cause for the shift is not likely to be protonation but a change in environment due to the formation of Q_B^-.

The FTIR difference spectra due to the $Q_B \rightarrow Q_B^-$ reaction may provide information about the role of conformational changes. The X-ray crystal structures of RCs frozen in the dark (PQ_B) state and in the light ($P^+Q_B^-$) state show a 5 Å movement of Q_B from a distal position to a proximal position (*5*). FTIR studies by Breton et al. do not show a change in the spectrum of the quinone and indicate that the position of the quinone does not change upon reduction at 15 °C (*61*). If the movement of Q_B occurs, many more water molecules would be expected to exhibit structural changes. If Q_B were

[2] We concluded that positive peaks contain water vibrations for EQ-L212 (Figures 3c and 4c), but not for WT (Figures 3b and 4b). However, the signal amplitudes were similar at 2800−2400 cm^{-1} in H_2O (Figure 3b,c). In the case of the X−D stretching region, the signal of EQ-L212 was even smaller than that of WT (Figure 4b,c). While the reason is unclear at present, the mutation at Glu-L212 may influence the vibrations except water, such as N−H stretching vibrations at His-L190. Identification of these bands is our future focus.

to move by 5 Å, we would expect to observe more than two O−H group shifts. This supports previous FTIR results which suggest a proximal position for neutral Q_B at room temperature (*61*). However, it should be noted that water molecules displaced by Q_B^- movement may be more strongly hydrogen bonded and consequently may not be observed in this study.

Changes due to weakly hydrogen bonded water molecules were observed due to formation of Q_A^-. In the weakly hydrogen bonded region of the spectrum after transfer of an electron to Q_A, one band was found to appear and three bands were found to disappear. The structure around Q_A is relatively hydrophobic, and there are a smaller number of water molecules in the X-ray crystal structure (*3*−*6*). In addition, there may be weakly hydrogen bonded water molecules near Q_A that may not be well-ordered and thus not observed by X-ray crystallography. The reorientation of the weakly hydrogen bonded water protons may help stabilize the charge on Q_A^-. A conformational change due to water reorientation may explain the changes in recombination kinetics observed for RCs frozen in the light or frozen in the dark (*62*).

Weakly hydrogen bonded water molecules have also been detected by FTIR in PSII associated with the S_1 to S_2 electron transfer reaction of the water-oxidizing complex (*46*) and oxidation of the redox active tyrosine Y_D (*63*). Weakly hydrogen bonded water molecules lack strong hydrogen bonds that fix them in position and should be able to reorient in the electric field of the cofactor following electron transfer. These water molecules are uniquely able to stabilize charges formed by electron transfer by dielectric screening resulting from the reoriented water dipole. Thus, weakly hydrogen bonded water molecules may play a special role in stabilizing charge-separated states in proteins.

CONCLUSIONS

FTIR spectroscopy and ^{18}O water substitution can be used to identify water molecules perturbed by electron transfer to Q_A and Q_B in bacterial RCs. An FTIR band near 2100 cm^{-1} in D_2O due to electron transfer forming Q_B^- in the EQ-L212 mutant RC was shifted by ^{18}O water substitution and could conceivably be due to protonation of a water molecule. This result is consistent with the idea that protonated water molecules can be stable components in a proton transfer pathway. Isotope-shifted bands were observed in RCs due to formation of Q_A^- and Q_B^- in the spectral region of 3700−3500 cm^{-1} characteristic of weakly hydrogen bonded water molecules. The changes due to Q_B^- are due to water molecules near Glu-L212. These results show that water molecules near the quinone sites are present and are perturbed by the charge on the quinone. These weakly hydrogen bonded water molecules may be important for stabilizing the charge on the quinone and facilitate transfer of a proton to the Q_B site.

REFERENCES

1. Okamura, M. Y., and Feher, G. (1992) Proton transfer in reaction centers from photosynthetic bacteria. *Annu. Rev. Biochem. 61*, 861–896.
2. Okamura, M. Y., Paddock, M. L., Graige, M. S., and Feher, G. (2000) Proton and electron transfer in bacterial reaction centers. *Biochim. Biophys. Acta 1458*, 148–163.
3. Ermler, U., Fritzsch, G., Buchanan, S. K., and Michel, H. (1994) Structure of the photosynthetic reaction center from *Rhodobacter sphaeroides* at 2.65 Å resolution: Cofactors and protein-cofactor interactions. *Structure 2*, 925–936.
4. Stowell, M. H. B., McPhillips, T. M., Rees, D. C., Soltis, S. M., Abresch, E., and Feher, G. (1997) Light-induced structural changes in photosynthetic reaction center: Implications for mechanism of electron-proton transfer. *Science 276*, 812–816.
5. Axelrod, H. L., Abresch, E. C., Paddock, M. L., Okamura, M. Y., and Feher, G. (2000) Determination of the binding sites of the proton transfer inhibitors Cd^{2+} and Zn^{2+} in bacterial reaction centers. *Proc. Natl. Acad. Sci. U.S.A. 97*, 1542–1547.
6. Lancaster, C. R. D., and Michel, H. (1997) The coupling of light-induced electron transfer and proton uptake as derived from crystal structures of reaction centers from *Rhodopseudomonas viridis* modified at the binding site of the secondary quinone, Q_B. *Structure 5*, 1339–1359.
7. Paddock, M. L., Rongey, S. H., Feher, G., and Okamura, M. Y. (1989) Pathway of proton transfer in bacterial reaction centers: Replacement of glutamic acid 212 in the L subunit by glutamine inhibits quinone (secondary acceptor) turnover. *Proc. Natl. Acad. Sci. U.S.A. 86*, 6602–6606.
8. Takahashi, E., and Wraight, C. A. (1992) Proton and electron transfer in the acceptor quinone complex of *Rhodobacter sphaeroides* reaction centers: Characterization of site-directed mutants of the two ionizable residues, Glu^{L212} and Asp^{L213}, in the Q_B binding site. *Biochemistry 31*, 855–866.
9. Shinkarev, V. P., Takahashi, E., and Wraight, C. A. (1993) Flash-induced electric potential generation in wild type and L212EQ mutant chromatophores of *Rhodobacter sphaeroides*: QBH2 is not released from L212EQ mutant reaction centers. *Biochim. Biophys. Acta 1142*, 214–216.
10. Takahashi, E., and Wraight, C. A. (1990) A crucial role of Asp^{L213} in the proton transfer pathway to the secondary quinone of reaction centers from *Rhodobacter sphaeroides*. *Biochim. Biophys. Acta 1020*, 107–111.
11. Paddock, M. L., Rongey, S. H., McPherson, P. H., Juth, A., Feher, G., and Okamura, M. Y. (1994) Pathway of proton transfer in bacterial reaction centers: Role of aspartate-L213 in proton transfers associated with reduction of quinone to dihydroquinone. *Biochemistry 33*, 734–745.
12. Paddock, M. L., McPherson, P. H., Feher, G., and Okamura, M. Y. (1990) Pathway of proton transfer in bacterial reaction centers: Replacement of serine-L223 by alanine inhibits electron and proton transfers associated with reduction of quinone to dihydroquinone. *Proc. Natl. Acad. Sci. U.S.A. 87*, 6803–6807.
13. Paddock, M. L., Feher, G., and Okamura, M. Y. (1995) Pathway of proton transfer in bacterial reaction centers: Further investigations on the role of Ser-L223 studied by site-directed mutagenesis. *Biochemistry 34*, 15742–15750.
14. Paddock, M. L., Äderloth, P., Chang, C., Abresch, E. C., Feher, G., and Okamura, M. Y. (2001) Identification of the proton pathway in bacterial reaction centers: Cooperation between Asp-M17 and Asp-L210 facilitates proton transfer to the secondary quinone (Q_B). *Biochemistry 40*, 6893–6902.
15. Äderloth, P., Paddock, M. L., Tehrani, A., Beatty, T., Feher, G., and Okamura, M. Y. (2001) Identification of the proton pathway in bacterial reaction centers: Decrease of proton transfer rate by mutation of surface Histidines at H126 and H128 and chemical rescue by imidazole identifies the initial proton donors. *Biochemistry 40*, 14538–14546.
16. Marrotti, P., and Wraight, C. A. (1988) Flash-induced H^+ binding by bacterial photosynthetic reaction centers: Influences of the redox states of the acceptor quinones and primary donor. *Biochim. Biophys. Acta 934*, 329–347.
17. McPherson, P. H., Okamura, M. Y., and Feher, G. (1988) Light-induced proton uptake by photosynthetic reaction centers from *Rhodobacter sphaeroides* R-26. I. Protonation of the one-electron states $D^+Q_A^-$, DQ_A^-, $D^+Q_AQ_B^-$ and $DQ_AQ_B^-$. *Biochim. Biophys. Acta 934*, 348–368.
18. Vermeglio, A. (1977) Secondary electron transfer in reaction centers of *Rhodopseudomonas sphaeroides*. Out-of-phase periodicity of two for the formation of ubisemiquinone and fully reduced ubiquinone. *Biochim. Biophys. Acta 459*, 516–524.
19. Wraight, C. A. (1977) Electron acceptors of photosynthetic bacterial reaction centers: Direct observation of oscillatory behaviour suggesting two closely equivalent ubiquinones. *Biochim. Biophys. Acta 459*, 525–531.

20. Nabedryk, E., and Breton, J. (2008) Coupling of electron transfer to proton uptake a the Q_B site of the bacterial reaction center: A perspective from FTIR spectroscopy. *Biochim. Biophys. Acta 1777*, 1229–1248.
21. Gunner, M. R., and Honig, B. (1992) Calculations of proton uptake in *Rhodobacter sphaeroides* reaction centers. In *The Photosynthetic Bacterial Reaction Center II* (Breton, J., and Verméglio, A., Eds.) pp 403−410, Plenum Press, New York.
22. Beroza, P., Fredkin, D. R., Okamura, M. Y., and Feher, G. (1995) Electrostatic calculations of amino acid titration and electron transfer, $Q_A^-Q_B \rightarrow Q_AQ_B^-$, in the reaction center. *Biophys. J. 68*, 2233–2250.
23. Lancaster, C. R. D., Michel, H., Honig, B., and Gunner, M. R. (1996) Calculated coupling of electron and proton transfer in the photosynthetic reaction center of *Rhodopseudomonas viridis*. *Biophys. J. 70*, 2469–2492.
24. Rabenstein, B., Ullmann, G. M., and Knapp, E.-W. (1998) Calculation of protonation patterns in proteins with structural relaxation and molecular ensembles: Application to the photosynthetic reaction center. *Eur. Biophys. J. 27*, 626–637.
25. Rabenstein, B., Ullmann, G. M., and Knapp, E.-W. (1998) Energetics of electron-transfer and protonation reactions of the quinones in the photosynthetic reaction center of *Rhodopseudomonas viridis*. *Biochemistry 37*, 2488–2495.
26. Alexov, E. G., and Gunner, M. R. (1999) Calculated protein and proton motions coupled to electron transfer: Electron transfer from Q_A^- to Q_B in bacterial photosynthetic reaction centers. *Biochemistry 38*, 8253–8270.
27. Nabedryk, E., Breton, J., Hienerwadel, R., Fogel, C., Paddock, M. L., and Okamura, M. Y. (1995) Fourier transform infrared difference spectroscopy of secondary quinone acceptor photoreduction in proton transfer mutants of *Rhodobacter sphaeroides*. *Biochemistry 34*, 14722–14732.
28. Nabedryk, E., Breton, J., Okamura, M. Y., and Paddock, M. L. (1998) Proton uptake by carboxylic acid groups upon photoreduction of the secondary quinone (Q_B) in bacterial reaction centers from *Rhodobacter sphaeroides*: FTIR studies on the effects of replacing Glu H173. *Biochemistry 37*, 14457–14462.
29. Nabedryk, E., Breton, J., Okamura, M. Y., and Paddock, M. L. (1998) Direct evidence of structural changes in reaction centers of *Rb. sphaeroides* containing suppressor mutations for Asp L213 → Asn: A FTIR study of Q_B photoreduction. *Photosynth. Res. 55*, 293–299.
30. Nabedryk, E., Breton, J., Okamura, M. Y., and Paddock, M. L. (2001) Simultaneous replacement of Asp-L210 and Asp-M17 with Asn increases proton uptake by Glu-L212 upon first electron transfer to Q_B in reaction centers from *Rhodobacter sphaeroides*. *Biochemistry 40*, 13826–13832.
31. Nabedryk, E., Breton, J., Okamura, M. Y., and Paddock, M. L. (2004) Identification of a novel protonation pattern for carboxylic acids upon Q_B photoreduction in *Rhodobacter sphaeroides* reaction center mutants at Asp-L213 and Glu-L212 sites. *Biochemistry 43*, 7236–7243.
32. Takahashi, E., and Wraight, C. A. (1992) Proton and electron transfer in the acceptor quinone complex of *Rhodobacter sphaeroides* reaction centers: Characterization of site-directed mutants of the two ionizable residues, Glu^{L212} and Asp^{L213}, in the Q_B binding site. *Biochemistry 31*, 855–866.
33. Breton, J., Nabedryk, E., Mioskowski, C., and Boullais, C. (1996) Protein-quinone interactions in photosynthetic bacterial reaction centers investigated by light-induced FTIR difference spectroscopy. In *The Reaction Center of Photosynthetic Bacteria, Structure and Dynamics* (Michel-Beyerle, M.-E., Ed.) pp 381−394, Springer-Verlag, New York.
34. Eigen, M. (1964) Proton transfer, acid-base catalysis, and enzymatic hydrolysis. Part I: Elementary processes. *Angew. Chem., Int. Ed. 3*, 1–19.
35. Zundel, G. (1976) in *The Hydrogen Bond: Recent Developments in Theory and Experiments* (Schuster, P., Zundel, G., and Sandorfy, C., Eds.) pp 687−766, North-Holland, Amsterdam.
36. Breton, J., and Nabedryk, E. (1998) Proton uptake upon quinone reduction in bacterial reaction centers: IR signature and possible participation of a highly polarizable hydrogen bond network. *Photosynth. Res. 55*, 301–307.
37. Hermes, S., Stachink, J. M., Onidas, D., Remy, A., Hofmann, E., and Gerwert, K. (2006) Proton uptake in the reaction center mutant L210DN from *Rhodobacter sphaeroides* via protonated water molecules. *Biochemistry 45*, 13741–13749.
38. Rammelsberg, R., Huhn, G., Lübben, M., and Gerwert, K. (1998) Bacteriorhodopsin's intramolecular proton-release pathway consists of a hydrogen-bonded network. *Biochemistry 37*, 5001–5009.
39. Garczarek, F., Brown, L. S., Lanyi, J. K., and Gerwert, K. (2005) Proton binding within a membrane protein by a protonated water cluster. *Proc. Natl. Acad. Sci. U.S.A. 102*, 3633–3638.
40. Kandori, H., and Shichida, Y. (2000) Direct observation of the bridged water stretching vibrations inside a protein. *J. Am. Chem. Soc. 122*, 11745–11746.
41. Shibata, M., Tanimoto, T., and Kandori, H. (2003) Water molecules in the schiff base region of bacteriorhodopsin. *J. Am. Chem. Soc. 125*, 13312–13313.
42. Shibata, M., and Kandori, H. (2005) FTIR studies of internal water molecules in the Schiff base region of bacteriorhodopsin. *Biochemistry 44*, 7406–7413.
43. Lórentz-Fonfria, V. A., Furutani, Y., and Kandori, H. (2008) Active internal water in the bacteriorhodopsin photocycle. A comparative study of the L and M intermediates at room and cryogenic temperatures by infrared spectroscopy. *Biochemistry 47*, 4071–4081.
44. Kandori, H. (2000) Role of internal water molecules in bacteriorhodopsin. *Biochim. Biophys. Acta 1460*, 177–191.
45. Furutani, Y., Shibata, M., and Kandori, H. (2005) Strongly hydrogen-bonded water molecules in the Schiff base region of rhodopsins. *Photochem. Photobiol. Sci. 4*, 661–666.
46. Noguchi, T., and Sugiura, M. (2002) Flash-induced FTIR difference spectra of the water oxidizing complex in moderately hydrated photosynthetic II core films: Effect of hydration extent on S-state transmission. *Biochemistry 41*, 2322–2330.
47. Breton, J., Thibodeau, D. L., Berthomieu, C., Mäntele, W., Verméglio, A., and Nabedryk, E. (1991) Probing the primary quinone environment in photosynthesis bacterial reaction centers by light-induced FTIR difference spectroscopy. *FEBS Lett. 278*, 257–260.
48. Breton, J., Berthomieu, C., Thibodeau, D. L., and Nabedryk, E. (1991) Probing the secondary quinone (Q_B) environment in photosynthesis bacterial reaction centers by light-induced FTIR difference spectroscopy. *FEBS Lett. 288*, 109–113.
49. Breton, J., Boullais, C., Burie, J.-R., Nabedryk, E., and Mioskowski, C. (1994) Binding sites of quinones in photosynthetic bacterial reaction centers investigated by light-induced FTIR difference spectroscopy: Assignment of the interactions of each carbonyl of Q_A in *Rhodobacter sphaeroides* using site-specific ^{13}C-labeled ubiquinone. *Biochemistry 33*, 14378–14386.
50. Brudeler, R., de Groot, H. J. M., van Liemt, W. B. S., Steggrerda, W. F., Esmeijer, R., Gast, P., Hoff, A. J., Lugtenburg, J., and Gerwert, K. (1994) Asymmetric binding of the 1- and 4-C═O groups of Q_A in *Rhodobacter sphaeroides* R26 reaction centers monitored by Fourier transform infrared spectroscopy using site-specific isotopically labeled ubiquinone-10. *EMBO J. 13*, 5523–5530.
51. Breton, J., Nabedryk, E., Allen, J. P., and Williams, J. C. (1997) Electrostatic influence of Q_A reduction on the IR vibrational mode of the 10a-ester C═O of H_A demonstrated by mutations at residues Glu L104 and Trp L100 in reaction centers from *Rhodobacter sphaeroides*. *Biochemistry 36*, 4515–4525.
52. Breton, J., Boullais, C., Berger, G., Mioskowski, C., and Nabedryk, E. (1995) Binding sites of quinones in photosynthetic bacterial reaction centers investigated by light-induced FTIR difference spectroscopy: Symmetry of the carbonyl interactions and close equivalence of the Q_B vibrations in *Rhodobacter sphaeroides* and *Rhodopseudomonas viridis* probed by isotope labeling. *Biochemistry 34*, 11606–11616.
53. Brudler, R., de Groot, H. J. M., van Liemt, W. B. S., Gast, P., Hoff, A. J., Lugtenburg, J., and Gerwert, K. (1995) FTIR spectroscopy shows weak symmetric hydrogen bonding of the Q_B carbonyl groups in *Rhodobacter sphaeroides* R26 reaction centres. *FEBS Lett. 370*, 88–92.
54. Breton, J. (2007) Steady-state FTIR spectra of the photoreduction of Q_A and Q_B in *Rhodobacter sphaeroides* reaction centers provide evidence against the presence of a proposed transient electron acceptor X between the two quinones. *Biochemistry 46*, 4459–4465.
55. Nabedryk, E., Paddock, M. L., Okamura, M. Y., and Breton, J. (2005) An isotope-edited FTIR investigation of the role of Ser-L223 in binding quinone (Q_B) and semiquinone (Q_B^-) in the reaction center from *Rhodobacter sphaeroides*. *Biochemistry 44*, 14519–14527.

56. Okumura, M., Yeh, L. I., Myers, J. D., and Lee, Y. T. (1990) Infrared spectra of the solvated hydronium ion: Vibrational predissociation spectroscopy of mass-selected $H_3O^+ \cdot (H_2O)_n \cdot (H_2)_m$. *J. Phys. Chem. 94*, 3416–3427.
57. Headrick, J. M., Diken, E. G., Walters, R. S., Hammer, N. I., Christie, R. A., Cui, J., Myshakin, E. M., Duncan, M. A., Johnson, M. A., and Jordan, K. D. (2005) Structural signatures of hydrated proton vibrations in water clusters. *Science 308*, 1765–1769.
58. Kandori, H., Belenky, M., and Heltzfeld, J. (2002) Vibrational frequency and dipolar orientation of the protonated Schiff base in bacteriorhodopsin before and after photoisomerization. *Biochemistry 41*, 6026–6031.
59. Noguchi, T., Inoue, Y., and Tang, X.-S. (1999) Hydrogen bonding interaction between the primary quinone acceptor Q_A and a histidine side chain in photosystem II as revealed by Fourier transform infrared spectroscopy. *Biochemistry 38*, 399–403.
60. Breton, J., Lavergne, J., Wakeham, M. C., Nabedryk, E., and Jones, M. R. (2007) The unusually strong hydrogen bond between the carbonyl of Q_A and His M219 in the *Rhodobacter sphaeroides* reaction center is not essential for efficient electron transfer from Q_A^- to Q_B. *Biochemistry 46*, 6468–6476.
61. Breton, J., Boullais, C., Mioskowski, C., Sebban, P., Baciou, L., and Nabedryk, E. (2002) Vibrational spectroscopy favors a unique Q_B binding site at the proximal position in wild-type reaction centers and in the Pro-L209 → Tyr mutant from *Rhodobacter sphaeroides*. *Biochemistry 41*, 12921–12927.
62. Kleinfeld, D., Okamura, M. Y., and Feher, G. (1984) Electron-transfer kinetics in photosynthetic reaction centers cooled to cryogenic temperature in the charge-separated state: Evidence for light-induced structural changes. *Biochemistry 23*, 5780–5786.
63. Takahashi, R., Sugiura, M., and Noguchi, T. (2007) Water molecules coupled to the redox-active tyrosine Y_D in photosystem II as detected by FTIR spectroscopy. *Biochemistry 46*, 14245–14249.

BI801990S